Determining the circulation depth of thermal springs in the southern Rocky Mountain Trench, south-eastern British Columbia, Canada using geothermometry and borehole temperature logs

D. M. Allen · S. E. Grasby · D. A. Voormeij

Abstract Geochemical data for thermal spring waters along the southern Rocky Mountain Trench in British Columbia, Canada were examined. The range of equilibration temperatures for the thermal springs is between 24 and 59°C, assuming that there is minimal mixing with colder shallow waters that might lead to a lowering of the calculated equilibration temperature. The chalcedony geothermometer is found to be the most appropriate given the carbonate host rocks. Temperature logs from 11 boreholes in the vicinity were used to calculate representative geothermal gradients, which range from 23.8 to 55.7°C/km with an average of 24.8±8.0°C/km. Using the average gradient and the range of equilibration temperatures calculated for each spring, the minimum range for the depth of origin of the thermal waters is 0.9–2.2 km. Heat flow values range from 90.3 to 155 mW/m^2, with an average of 109.1±21.0 mW/m^2. The moderate to high heat flow and heat generation result in generally higher temperatures at shallow depths, thus offering an explanation for the occurrence of thermal springs. The alignment of the thermal springs likely relates to the preferred northwest–southeast orientation for major thrust faults along the Rocky Mountain Trench, and with waters routed from depth along deep faults.

Résumé Les données géothermiques de sources thermales le long de la partie sud du fossé des Montagnes Rocheuses en Colombie Britannique, Canada, sont étudiées. L'échelle des températures d'équilibre des sources thermales se situe entre 24 et 59°C, en assumant qu'il y a un mélange minimum avec les eaux froides de surface, ce qui conduit à une sous-évaluation de la température d'équilibre. La calcédoine apparaît être le géothermomètre le plus approprié vu les roches hôtes carbonatées. Les diagraphies de température provenant de 11 forages proches ont été utilisées pour calculer le gradient géothermique représentatif, gradient compris entre 23.8 et 55.7°/km avec une moyenne de 24.8°/km. En utilisant le gradient moyen et les valeurs de température d'équilibre calculées pour chaque source, la profondeur minimum des eaux thermales se situerait entre 0.9 et 2.2 km. Les flux de chaleur sont évalués entre 90.3 et 155 mW/m, avec une moyenne de 109.1±21.0 mW/m. Le transfert moyen de chaleur et la génération de chaleur résulte en températures ordinairement plus élevées aux faibles profondeurs, qui ainsi offre une explication à l'occurrence de sources thermales. Les alignements de sources thermales sont vraisemblablement en relation avec l'orientation Nord-Sud des principales failles-vraies le long du fossé des Montagnes Rocheuses, et avec l'écoulement des eaux des profondeurs le long des failles.

Resumen Se examinan datos geoquímicos de aguas de fuentes termales a lo largo de la Trinchera sur de las Montañas Rocosas en Columbia Británica, Canadá. El rango de temperaturas de equilibrio para las fuentes termales se encuentra entre 24 y 59°C, asumiendo que existe mezcla mínima con aguas someras más frías que podrían conducir a un descenso de la temperatura de equilibrio calculada. El geotermómetro de calcedonia se ha encontrado que es el más apropiado debido a las rocas encajonantes carbonatadas. Se utilizaron los registros de temperatura de 11 pozos de la zona para calcular gradientes geotermales representativos, los cuales varían de 23.8 a 55.7°C/km con un promedio de 24.8±8.0°C/km. Utilizando el gradiente promedio y el rango de temperaturas de equilibrio calculadas para cada manantial, se estimó que el rango mínimo para la profundidad de origen de las aguas termales varía de 0.9 a 2.2 km. Los valores de flujo de calor varían de 90.3 a 155 mW/m^2, con un promedio de 109.1±21.0 mW/m^2. El flujo de calor moderado a alto y la generación de calor resultan en temperaturas generalmente más altas a profundidades someras ofreciendo de este modo una explicación para la ocurrencia de fuentes termales. El alineamiento de fuentes

Received: 16 January 2004 / Accepted: 13 December 2004

D. M. Allen (✉) · D. A. Voormeij
Department of Earth Sciences,
Simon Fraser University,
8888 University Drive, Burnaby, British Columbia, Canada, V3Y 2L4
e-mail: dallen@sfu.ca
Tel.: +1-604-291-3967
Fax: +1-604-291-4198

S. E. Grasby
Geological Survey of Canada,
3303 - 33rd Street, Calgary, Alberta, Canada, T2L 2A7

Hydrogeol J (2006) 14:159–172 DOI 10.1007/s10040-004-0428-z

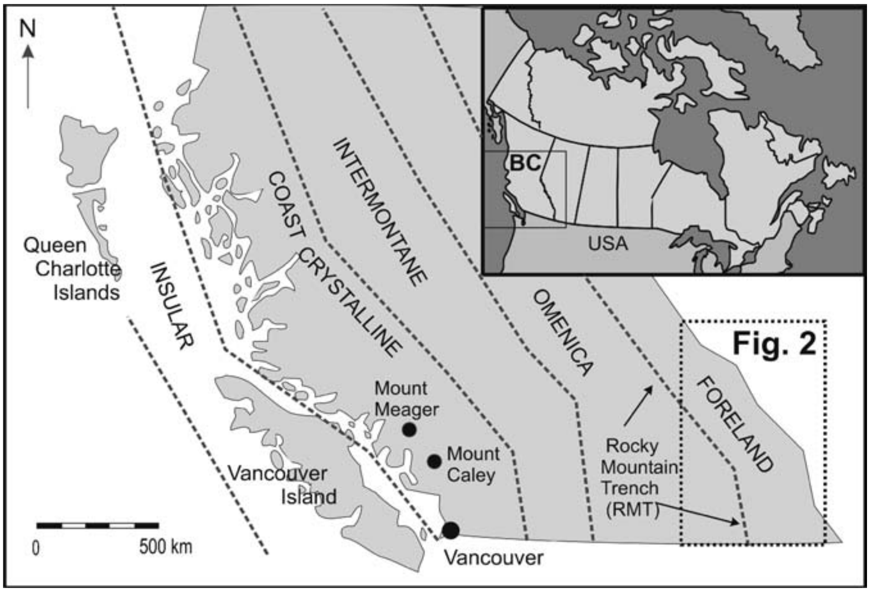

Fig. 1 Location map of the southern portion of the Province of British Columbia, Canada showing the tectonic belts of the Cordillera. Mount Meager and Mount Caley are known centers of recent volcanic activity. A high enthalpy geothermal energy resource exists beneath Mount Meager. Fig. 2 inset also shown

termales posiblemente se relaciona con la orientación preferida noroeste-sureste de fallas inversas principales a lo largo de la Trinchera de las Montañas Rocosas, y con aguas ascendentes profundas que se mueven a lo largo de fallas profundas.

Keywords Thermal springs · Hot springs · Geothermometry · Geothermal gradient heat flow · Rocky Mountain Trench · British Columbia · Canada

Introduction

Most thermal springs in Canada with temperatures above 10°C occur in the Cordilleran region. Souther and Halstead (1973) suggested that thermal springs are typically confined to the tectonically young Cordilleran region where high heat flow associated with young plutons may be responsible for thermal spring development. They noted that in many parts of British Columbia the springs also tend to occur in groups, each group being related to the same geological feature or the same flow system. Thus, the character and distribution of thermal waters in Canadian Cordillera were suspected to be closely related to regional topographic and geologic features, which control the circulation of groundwater, and hence, influence the temperature and chemistry of the water issuing from springs.

Grasby and Hutcheon (2001) showed that while springs in the Coast Belt are associated with volcanism, Canada is unusual in that the majority of geothermal systems are not associated with recent igneous activity. Rather, they are typically associated with deep circulation systems associated with complex Eocene-age structural features (i.e., major crustal-scale faults) in areas of low to moderate heat flow.

Most early studies on thermal waters in Canada were concentrated in the Coast Crystalline Belt (Fig. 1), where the recent volcanic activity at Mount Meager and Mount Caley (Souther and Dellechaie 1984), combined with the fractured nature of the volcanics and high precipitation rates along the coast, have created an environment that contains some of the hottest spring waters in Canada (Jessop et al. 1984). Geochemical analyses of thermal springs at Mount Meager indicate contact with high-temperature rock (Souther 1976), and Mount Meager has also been explored extensively for high-enthalpy geothermal energy (Lewis et al. 1992). Thermal springs in the southern Rocky Mountains (Fig. 2) had not been the subject of extensive research until recent publication of work by Grasby and Hutcheon (2001), probably because the surface water temperatures suggested moderate to low reservoir temperatures, and as such, the area was not considered to be a potential source of geothermal energy.

Many of the thermal waters in the southern Rocky Mountain trench, including Fairmont, Lussier, Ram Creek and Fording Mountain thermal springs, were sampled for major ion chemistry, selected minor constituents (e.g., Li, Sr, I, Br), and selected stable isotopes in studies dating back to 1967 and 1969 (van Everdingen 1969, 1972). More recently, Grasby et al. (2000) reported on the chemistry of numerous thermal springs in the Cordillera, including those listed above. Grasby et al. (2000) demonstrated, using recent and historical data for selected springs, that the temperature and chemistry of individual springs are constant through time. A complete set of recent chemical data for the southern Rocky Mountain region are summarized in this paper.

A thermodynamic evaluation of the springs was undertaken by van Everdingen (1969) in order to determine the degree of saturation of the spring waters with respect to calcite, dolomite and gypsum. The results were compared with observations on the presence or absence of spring deposits and with the analyses of the mineralogy made for the deposits at Banff and Fairmont springs. In later work, van Everdingen (1972) described the local

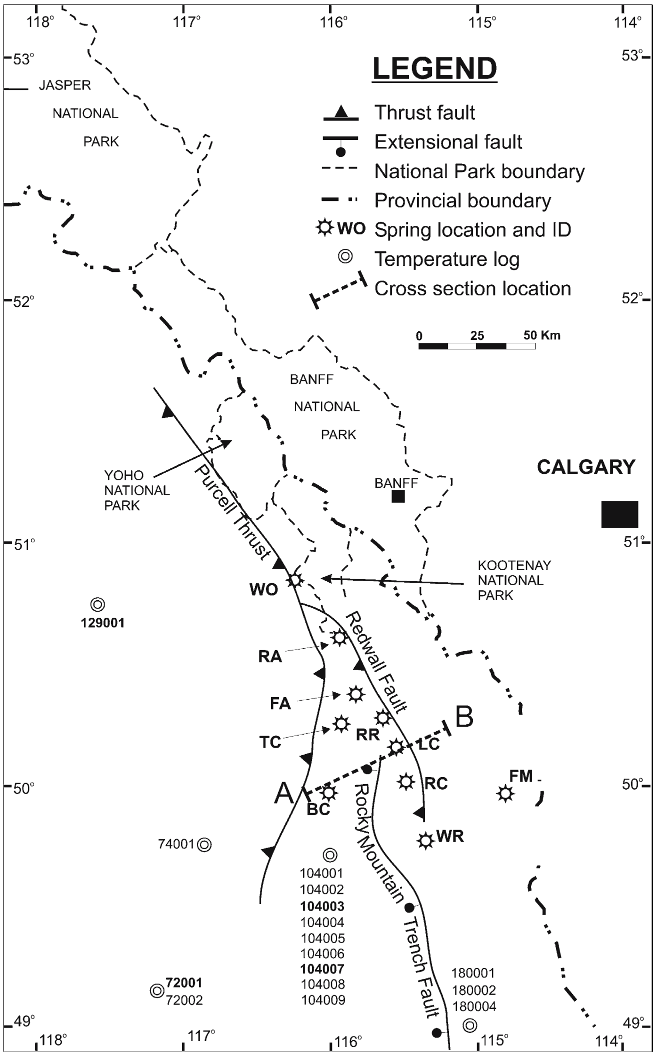

Fig. 2 Location map for the thermal springs and boreholes that were used for estimating geothermal gradients and heat flow (modified from van Everdingen 1969). Spring names are related to spring IDs in Table 1. Location of cross section line A–B for Fig. 3 is shown

geology and estimated the approximate depth of origin of the waters based on the measured spring temperatures at their source and an assumed geothermal gradient (33°C/km). The depths of circulation for these springs were estimated to be between 0.6 and 1.3 km, and the geological interpretation demonstrated that most springs issue from carbonate units. However, no reference was provided for the estimated geothermal gradient, and no geothermometric calculations were undertaken to estimate the reservoir temperatures based on observed chemistry.

More recently, Grasby et al. (2000) examined a number of chemical and stable isotope geothermometers for these thermal springs as part of a regional study to obtain estimates of subsurface temperatures. Again, minimum equilibration depth estimates were based on estimates of the regional thermal gradients. The southern Rocky Mountains were represented by a uniform geothermal gradient of 21°C/km (Hitchon 1984), yielding minimum equilibration depths of 1.7–3.3 km, with an average of 3±1 km.

The purpose of this paper is to determine the origin and circulation depth of thermal springs in the southern Rocky Mountain trench using geothermometry and borehole temperature logs. The available chemical database is used to describe spring chemistry, highlighting the similarities and differences of the various springs in the region, and to establish the chemical geothermometers necessary for determining equilibration temperatures of the spring waters. Temperature gradients measured in nearby boreholes are then used in conjunction with equilibration temperatures to estimate the depth of circulation of the thermal springs.

Study area

The Canadian Cordillera developed in response to the collision from Jurassic to Tertiary of island-arc terranes against the western margin of North America (Coney et al. 1980; Monger et al. 1982; Parrish et al. 1988; Gabrielse 1985; Gabrielse and Yorath 1989). The five morphogeological belts that comprise the Cordillera (Fig. 1) are roughly defined as deformed sedimentary strata of either North American (Foreland Belt) or island-arc affinity (Insular and Intermontane Belts), which are separated by belts of plutonic and high-grade metamorphic rocks (Coast and Omineca Belts). In response to the abrupt end of compressional deformation during the Late Paleocene, crustal-scale extensional faults formed in the southern Cordillera in association with plutonism and volcanism (Armstrong 1988; Parrish et al. 1988; Gabrielse and Yorath 1989). From Eocene to Recent, the south-western Cordillera has been affected by right-lateral strike-slip faulting (Gabrielse 1985). In addition, the Garibaldi volcanic belt (Fig. 2) developed from late Tertiary to Quaternary (Lewis and Souther 1978). Subduction and arc volcanism appear to have been continuous along the west coast at least since the Eocene (e.g., Hyndman et al. 1990).

The Rocky Mountain Trench is an anomalous, northwest–southeast-trending deep valley, which separates a belt of early Paleozoic and younger sedimentary rocks that have been folded and faulted on the east (Rocky Mountain Belt) from metamorphic, intrusive rocks and volcanics on the west (Omenica Belt). Due to poor exposure, the exact nature and origin of this structure is unclear. While having strike-slip motion in the northern portion (Price and Carmichael 1986), the southern Rocky Mountain Trench is characterized by a fault zone of Eocene and younger echelon, southwest-dipping normal faults (Price 1962; Bally et al. 1966; Clague 1974), with over 10 km of displacement (van der Velden and Cook 1994). Figure 3 shows a crustal-scale cross section through the southern Rocky Mountain trench showing the high-angle late-stage Rocky Mountain Trench Fault (after

DOI 10.1007/s10040-004-0428-z

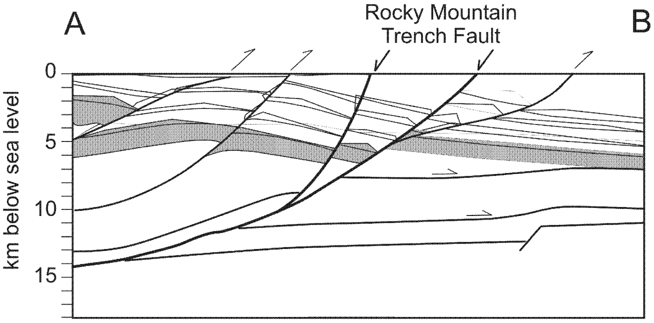

Fig. 3 Crustal-scale cross section through the southern Rocky Mountain trench showing the high-angle late-stage Rocky Mountain Trench Fault (modified from van der Velden 1995)

van der Velden 1995). At this latitude, it is splayed into two main fault systems. Note that it crosscuts earlier low-angle thrust faults reaching to the basement.

Thermal springs are only found in the southern portion of the Rocky Mountain Trench, with lower temperature springs in the valley bottom and higher temperature springs on the east side in a linear trend paralleling, and in between, the traces of the Southern Rocky Mountain Trench Fault Zone and the Redwall Fault (Fig. 2). The Redwall Fault is not well described in the literature; however, the east-verging back-rotated thrust fault is a significant structural boundary between the Porcupine Creek fan structure and the Purcell Anticlinorium (Foo 1979). Leech (1954) indicated that the fault has a component of late-stage, near-vertical, normal motion that is characterized by zones of brecciated carbonate. These springs have been attributed to flow within deep systems, and typically issue from layered carbonate rock within the Rocky Mountain Belt (van Everdingen 1972). Table 1 summarizes information on the location and local geology for each spring area.

Methodology

Water samples for selected springs in the study area were collected for chemical and isotopic analyses in 1967 and 1968 (van Everdingen 1969, 1972). Of the springs analyzed in that study, only two (Radium and Fairmont) had been previously reported (Satterley and Elworthy 1917). In 1993 and 2002, a subset of the same springs sampled by van Everdingen (i.e., the hottest ones at each site) plus additional springs not previously sampled were collected for chemical and isotopic analyses. The available chemical database is used to characterize spring chemistry throughout the southern Rocky Mountains and establish the chemical geothermometers necessary for determining equilibration temperatures of the spring waters. Temperature gradients measured in nearby boreholes are then used in conjunction with equilibration temperatures to estimate the depth of circulation of the thermal springs.

Chemical sampling and analysis

Spring samples collected in 1967 and 1968 are listed in Table 2. Unstable parameters (pH, redox potential, temperature, and specific conductance) were measured in-situ (van Everdingen 1972). pH and Eh were measured using a Corning Model 6 portable pH meter with millivolt meter, with Fisher #13-639-52 saturated calomel reference electrode; Fisher#13-639-102 platinum disc electrode; Sargent#S-30072-15 combination glass and reference electrode. Temperature was measured using an Atkins Technical Inc. Model 3L01 portable electronic thermometer, with thermistor probes, and specific conductance was measured using a Beckman Soulbridge type RB3-338 portable conductivity meter. Samples were submitted to the Western Regional Laboratory of the Water Quality Division, Inland Waters Branch, Calgary for chemical analysis. Whether the samples had been filtered and preserved in the field was not reported (discussed later).

Spring samples collected in 1993 and 2002 are designated with a sample ID with a suffix "–2" in Table 2. Unlike the earlier sampling where all issuing springs at a site were sampled, only the hottest spring was sampled. At many sites, several springs issue in close proximity (within tens of meters), and it can be assumed they represent a single hydrothermal system and that the hottest outlet represents the least amount of mixing with shallow ground water. Generally, water samples were collected less than 1 m from the rock face that forms the outlet. At Radium Hot Springs four closely-spaced springs are piped to a sump, where a bulk sample was collected. The Red Rock spring discharges into a side channel of the Kootenay River and is only assessable during periods of low water.

Unstable parameters (pH, temperature, redox potential, dissolved O_2, and HS^-) were measured in-situ. Dissolved O_2 and HS^- were measured using Chemetrics colorimetric kits. For the remaining analyses, samples were collected and preserved in the field. The water was passed through a 0.45-μm filter and acidified to pH <2 with ultrapure HNO_3 for cation analysis, and left untreated for anions. For SiO_2 determination, 10 ml of sample was diluted in the field with 50 ml of doubly distilled water. Samples were stored at 4°C.

Chemical and stable isotope analyses were conducted at the University of Calgary and the Geological Survey of Canada. Alkalinity was determined using an Orion 960 auto-titrator within 7 days of sample collection. Anions were measured by ion liquid chromatography, and cation concentrations were measured by flame atomic absorption. Analytical error in concentration measurements was estimated to be less than 2%. Charge balances are all less then 5%. All chemical calculations, including those for saturation index (SI) were undertaken using Solmineq88, a solution and mineral equilibrium code (Wiwchar et al. 1988). The (SI) is the logarithm of the ion activity product (IAP) divided by the equilibrium constant (*K*); negative

Table 1 Spring ID, spring name, location (as latitude and longitude) and elevation in meters above sea level (m.a.s.l.); summary of geological, structural and morphological location of the springs

Spring ID	Spring name	Latitude	Longitude	Elevation (m.a.s.l)	Spring location and description of local geology
WO 1	Wolfenden	50°50	116°16	850	Water discharges from an artesian well in the Columbia Valley bottom in an area underlain by over 2 m of peat and glacial sediments
RA 1	Radium[a]	50°38	116°02	1,005	Springs issue from Cambrian age dolomites of the Jubilee Formation adjacent to a normal fault. The four outlets have been covered and the water flow is directed into a sump for a public bathing pool
FA 5, 6, 10 FB 5, 6 FC 5, 6, 10 FD 6, 10	Fairmont[a]	50°20	115°54	1,040 888 1,022 1,027	Springs issue from Cambrian age dolomites of the Jubilee Formation (Souther and Halstead 1973). The springs are located in the sharp corner of the fault block near the point of intersection or merging of two normal faults. Travertine deposits several meters in thickness are located around the hottest of the Fairmont Springs (FA 5, 6 and 10) on Emanation Hill. Other springs occur at lower elevation and tend to be cooler
TC 1	Toby Creek	50°25	116°19	1,230	Springs issue from bedrock from the steep bank of Delphine Creek near the confluence of Toby Creek, and form large travertine deposits right above creek level. The springs occur in the faulted core of a regional anticline, in bedrock dominated by the Hardynian Dutch Creek Formation, dominantly argillite and slate
BC 1	Buhl Creek (Skookumchuck)[b]	49°58	116°02	1,250	Springs issue from gravels on the banks at the confluence of Buhl and Skookumchuck Creeks, and form several shallow pools at river level. There are no precipitates present. The bedrock is not exposed in the area but has been mapped as Cretaceous granites. The springs fall along the projection of the Hall Lake Fault, a major crustal scale feature
RR 1	Red Rock[b]	50°13	115°42	850	Springs issue from the sand and gravel river bank north of Lussier Springs on the Kootenay River just east of Canal Flats and form a large pool with active gas discharge. The water forms a small creek that flows directly into the Kootenay River
LC 7	Lussier Canyon (Whiteswan)[a]	50°08	115°35	1,167	Springs issue from the contact between Ordovician age limestone of the Beaverfoot and Brisco Formations that is associated with a steeply dipping transverse fault. The springs are located near the valley bottom and issue directly into the Lussier River north of Sharktooth Mountain
RC 7	Ram Creek[a]	50°02	115°35	1,457	Springs issue from a number of outlets on the north side of the small creek about 300 m upstream on the highest northern tributary of Ram Creek and Lussier River. Springs issue along the base of a wall of massive dolomitic limestone of Cambrian age of the Jubilee Formation. The springs are also situated downslope from the surface trace of a steeply dipping transverse fault, just like the Lussier springs, and are near the contact between the massive Upper-Jubilee and laminated Lower-Jubilee dolomites
FMa, FMb	Fording Mountain[a]	49°58	114°52	1,240	Springs issue from Permian-Pennsylvanian Rocky Mountain Formation on the west flank of the Fording Mountain anticline between Fording Mountain and the Elk River. Geology consists of an upper sequence of dolomite, shale, chert, conglomerate and sandstones, and a lower sequence of mainly calcareous and quartzitic sandstones. The Rocky Mountain Formation is underlain by the limestones, dolomitic limestones, dolomite and siltstone of the Rundle Group, which contains anyhydrite in the upper units
WH 1	Wild Horse[b]	49°48	115°30	1,610	There are both cold and warm springs at this location. Cold springs issue from various sources and merge to form a single cool creek near Wild Horse River. A large cold spring also flows into the spring at the base of the tufa. Warmer water flows from at least six vents on a metre-high tufa bench into the river

[a] Descriptions from van Everdingen (1969, 1972)

[b] Descriptions from Woodsworth (1999)

DOI 10.1007/s10040-004-0428-z

Table 2 Selected hydrochemical[a] and isotopic[b] parameters

Spring ID	Sampling date	pH[c]	Eh (mV)	Conductivity at 25°C (μmhos/cm)	TDS (mg/l)	Temperature (°C)	Ca	Sr	Mg	Na	K	Fe	Mn	Cu	Zn	Li
WO 1-2	10/1/1993	6.77			1,096.7	27.7	120	1.8	84.7	48.4	4.6	0.111	0.850			0.017
RA 1	6/28/1968	6.8				45.1	144.1		32	15.0	3.0					
RA 1-2	11/15/1993	6.69	+518		827.8	44.0	150	1.6	33.2	14.9	3.27	0.031	0.012	0.007	0.024	0.040
FA 5	5/25/1967	6.8[c]		2,480		45.7	484.8		105.2	31.3	6.2					
FA 6	6/27/1968	6.05	+330	2,360		45.9	430.7	3.6	113.2	32.1	5.9					0.049
FA 10	10/18/1967	7.0[c]		2,430		48.9	472.8		112.2	31.1	5.6	0.030	0.037	0.017	0.062	
FA 10-2	10/1/1993	6.25	+468		2,276.9	46.7	451	3.51	107	29.0	5.5	0.027	0.038	0.012	0.069	0.044
FB 5	5/25/1967	6.8[c]		2,530		31.6	480.8		110.2	31.7	6.8					
FB 6	6/27/1968	6.3	+412	2,450		32.0	413.6	3.5	115.2	33.0	6.1					0.053
FC 5	5/25/1967	6.8[c]		2,050		42.2	372.5		88.1	23.7	4.4					
FC 6	6/27/1968	6.1	+416	1,950		34.8	330.4	2.6	88.1	22.5	4.3					0.037
FC 10	10/18/1967	6.8[c]		1,800		41.8	314.4		83.1	19.9	3.6	0.080	0.045	0.015	0.039	
FD 6	6/27/1968	8.25	+420	220		8.5	23	0.1	14	0.8	0.4					<0.005
FD 10	10/18/1967	8.3[c]		271		4.8	31		17	0.6	0.4	0.030	0.007	<0.005	<0.005	
TC 1-2	10/1/1993	6.28	263.6		3,068.0	8.9	509	2.1	124.0	137.0	5.9	0.040	0.899	0.012	0.019	0.148
BC-2	5/11/2002	8.15	+151		243.7	32.5	7.2	0.10	0.39	59.0	2.2		0.0005	0.0004		0.14
RR 1-2	11/5/2002	6.30	+185		1,199.3	18.3	220	<.001	59	10.0	2.4	0.006	0.0006	0.0004	0.021	0.019
LC 7	7/3/1968	7.1	−88	5,220		43.4	145.3	1.0	25	876.7	10.0					
LC 7-2	10/1/1993	7.07	−51		2,937.1	43.2	115	1.09	24.8	979.0	10.6	0.023	0.008	0.006	0.016	0.080
RC 7	7/3/1968	7.6		400		34.6	50	0.2	15	2.6	1.3					
RC 7-2	10/1/1993	7.68	+481		294.0	36.5	49.2	0.2	14.5	2.4	1.3	<.005	0.004	<.003	0.005	0.002
FMa	7/2/1968	7.1	−176	3,710		24.7	345.6	6.5	95.2	344.7	16.8					0.82
FMb	7/2/1968	7.12	−246	3,710		25.9	375.7	6.2	95.1	344.7	16.6					0.82
FMb-2	11/1/1993	7.15	−236		3,051.0	20.5	375	16.8	104	423.0	18.6	0.083	0.014	0.011	0.003	0.921
WR 1-2	10/1/1993	7.13	+537		1,628.7	31.0	378	2.6	59.5	5.9	6.2	0.032	0.013	0.012	0.009	0.023

values indicate under-saturation and positive values, over-saturation.

Stable isotope ratios ($^{18}O/^{16}O$, D/H and $^{34}S/^{32}S$) are expressed using the usual δ notation:

$$\delta\,(\%) = \left(\frac{R_{\mathrm{sample}} - R_{\mathrm{standard}}}{R_{\mathrm{standard}}}\right) \times 10^3 \tag{1}$$

where R is the ratio of the heavy to light isotope abundances. The standards used are V-SMOW for oxygen and hydrogen and V-CDT for sulphur. $\delta^{18}O_{(H2O)}$ was measured on CO_2 isotopically equilibrated with H_2O (Epstein and Mayeda 1953), and δD was measured using H_2 produced by the Zn-reduction method (Coleman et al. 1982). For $\delta^{34}S$ analyses, SO_2 was prepared using the methods of Yanagisawa and Sakei (1983), $\delta^{18}O(SO_4)$ was measured with CO_2 prepared by graphite reduction of $BaSO_4$ (Shakur 1982). Combined sampling and analytical errors for isotope data were estimated to be ±0.2% for $\delta^{18}O_{(H2O)}$ and $\delta^{34}S$, and ±1% for δ^2H and $\delta^{18}O(SO_4)$.

Because of the uncertainty in quality assurance and quality control for the early samples, particularly with regard to sample dilution for SiO_2 analysis, only the 1993/2002 data are used for geothermometric calculations. However, for general discussion of chemical characteristics of the spring waters, the entire database is considered because it supports the fact that spring chemistry is relatively stable over time.

Geothermometry

Chemical geothermometry is an important tool in evaluating geothermal resources and exploring the potential source temperatures for thermal springs. A fundamental assumption of geothermometry, from the perspective of estimating the equilibration temperatures for thermal waters, is that the effects of dilution from surface and/or shallow groundwaters are insignificant and that thermodynamic equilibrium has been attained (Fournier 1981). Geothermometric calculations are based on the assumption that groundwater equilibrates with minerals in the reservoir rock. The concentrations of various ions (e.g., Na^+, K^+ and Ca^{2+}) and silica (SiO_2) are temperature-dependent, and reactions with the circulating aqueous solutions are typically sluggish (Yorath et al. 1991). Therefore, for relatively rapid transit times to the surface, such as would be accomplished along fracture zones, it is unlikely that re-equilibration with the surrounding rocks could occur.

There are many types of geothermometers; some more suitable than others for different types of temperature conditions. In general, geothermometers based on ratios are more resistant to dilution effects than those based on absolute concentrations (Banks et al. 1998). However, caution must be taken in choosing an appropriate geothermometer. The silica, Na/K and Na–Ca–K geothermometers are expected to be most appropriate for the range of temperature conditions found in springs within the southern Rocky Mountains region (Banks et al. 1998). However, the presence of carbonate host rocks in the study area complicates the selection of an appropriate geothermometer.

The following geothermometers were applied to the available chemical data: Chalcedony (Fournier 1977), Quartz (Fournier 1977), Na/K (Fournier 1973), Na–K–Ca (Fournier and Truesdell 1973), Na–K–Ca (Mg corrected) (Fournier 1979), and Mg/Li (Kharaka and Mariner 1988). The temperatures for the springs in the study area are likely too low for equilibrium exchange of oxygen isotopes between SO_4–H_2O to occur rapidly enough at the pH of the springs (Chiba and Sakai 1985) making the geothermometer of Mizutani and Rafter (1969) invalid.

Temperature logs

Regional geothermal gradients were obtained from the Canadian geothermal database, which has recently been assembled by A.M. Jessop (personal communication) and

Table 2 continued

HCO_3	SO_4	Cl	I	Br	F	PO_4	NO_3	SiO_2	H_2S	CO_2	O_2	CBE (%)	$\delta^{18}O_{H2O}$ (‰)	$\delta^{2}H_{H2O}$ (‰)	$\delta^{34}S_{SO4}$ (‰)	$\delta^{18}O_{SO4}$ (‰)
531	210	78.0				0	4.5	18.2				−0.29	−19.1	−147	9.6	
206.1	319.1	10.8										1.08				
217	356	13.2			<1	<2	<1	38.6	0		2.9	−1.56	−18.8	−154	18.8	10.5
710.2	1,010.7	40.6			1.50		0.3	38.0				0.66				
714.2	985.6	33.1	0.008	<0.1			0.2	31.0	0	400	0.6	−1.10				
700.2	991.6	52.0			0.81	0.19	<0.1	34.1				1.01				
685	929	34.0			<1	<2	<1	32.9	0		2.5	1.97	−18.8	−145	17.7	13.0
709.2	1,014.7	44.1			1.30		0.4	35.3				0.79				
704.1	897.4	34.6	0.006	<0.1			0.1	32.0	0	240	1.3	0.94				
627.8	775	33.0			0.98		0.4	27.3				−0.80				
585.7	682.8	25.0	0.002	<0.1			0.3	24.0	0	450	0.7	0.74				
559.6	628.7	27.0			0.58	0.12	0.3	21.0				0.91				
134	10	<0.1	0.005	<0.1			0.2	3.7	0	0.0	11.0	−1.27				
165	11	0.2			0.07	0.02	0.4	6.4				0.57				
1307	900	13.0			<1	<2	<1	70.0				3.38	−19.0	−160	30.4	11.4
92	46	10.8						26.0	0		0.3	4.59		−159	8.9	
511	379	11.9						6.0	0		3.2	−.82		−140	18.0	
218.4	135.3	1,404.8	0.015			0.2	0.05	36.0	2	20	0	1.81				
222	148	1,400.0			<1	1.90	0.52	36.6	32		0.75	4.53	−18.3	−145	20.5	7.3
155	57	1.7					0.5	21.0	0	5	5.4	1.26				
148	56	1.2			<1	<2	<1	21.3	0		4.8	4.53	−17.3	−141	18.0	5.8
207.4	1,432.8	305.6	0.098	0.6		0.1	0.05	16.0	70	65	0	−1.31				
245.5	1,372.6	305.6	0.08	0.5		0.11	0.1	14.0	60	60	0	1.23				
268.7	1,483	355.9						16.8				1.46	−19.9	−154	24.7	
105.3	1,038.2	2.4			0.7		0.21	30.7	0.0		1.5	1.65	−18.7	−138	20.3	17.5

Spring IDs (from Table 1) in bold face are representative samples for geothermometry calculations as these either have the highest temperatures at each site or are the only sample for that site

[a] Ion and gas concentrations in mg/l

[b] Stable isotope concentrations for O and H measured relative to V-SMOW; for S measured relative to V-CDT

[c] pH measured in laboratory

will be published by the Geological Survey of Canada. This database expands the temperature, thermal conductivity, heat generation, and heat flow data assembled for various regions across Canada. A compilation for the Canadian Cordillera was undertaken by Lewis (1991) and was supplemented by Lewis et al. (1992), and serves as reference for our calculations. Generally, the logs were obtained from boreholes of opportunity (e.g., mining boreholes), but on occasion, from research boreholes.

In the study region, there are 13 available temperature logs in the database; only 11 provide good records of the geothermal gradient. Figure 2 shows the location of the boreholes and highlights in bold the most representative temperature log where data from more than one borehole at the location are available. Temperatures were measured with a high-resolution and high-accuracy portable temperature logging system. The depth interval between temperature measurements is typically 15 m. Some of the logs are shallow (up to 30 m in depth), while the majority extend 1,300 m in depth.

Results

Major ion chemistry

Chemical data for all samples are provided in Table 2. The charge balance error for all samples (CBE in Table 2) are within a highly acceptable range (−1.56 to +4.59%), giving confidence that the analysis results are suitable for general geochemical interpretation. Worth noting is the similarity between the chemical compositions of spring waters sampled in the late 1960s and early 1970s and the same springs in the 1990s and early 2000 (i.e., RA 1, FA 10, LC 7, RC 7 and FMb in Table 2). These results demonstrate that the springs are relatively stable in chemical composition over this time frame, and provide some support for using van Everdingen's 1969 and 1972 data when later data are lacking.

The relative abundance of major cation and anion constituents varies considerably across the region. These relative abundance changes are visually represented on Stiff diagrams (Stiff 1951), in which cation concentrations (in milliequivalents per liter) are plotted on the left of a vertical zero axis and anion concentrations on the right (Fig. 4). Waters are classified according to hydrochemical facies. The facies are a function of the lithology, solution kinetics, and flow patterns of the aquifer (Back 1966). Here, waters are arbitrarily assigned Type I, Type II, etc.

Type I waters (Ca–Mg–SO_4–HCO_3) include all samples collected from FA, FB, and FC as well as RA and WR 1. Type I waters have high Ca relative to Mg, low Na, and high SO_4 relative to either HCO_3 or Cl (the high Ca and SO_4 may be indicative of gypsum dissolution). These springs are hosted in carbonate rocks, consisting dominantly of dolomites, with only occasional limestone. Sample WR 1 has a slightly lower HCO_3 concentration relative to SO_4 compared to the other Type I waters.

Type II waters (Ca/Mg–SO_4–HCO_3) include the two FD samples. These are similar to Type I waters except that Ca and Mg are in approximately equal proportions (higher Mg may indicate dedolimitization) and the relative SO_4 concentration is low. Type III waters include RC, RR and TC, and Type IV includes WO. These two water types have either Ca or Mg as the dominant cation, and HCO_3 rather than SO_4 as the dominant anion. Finally,

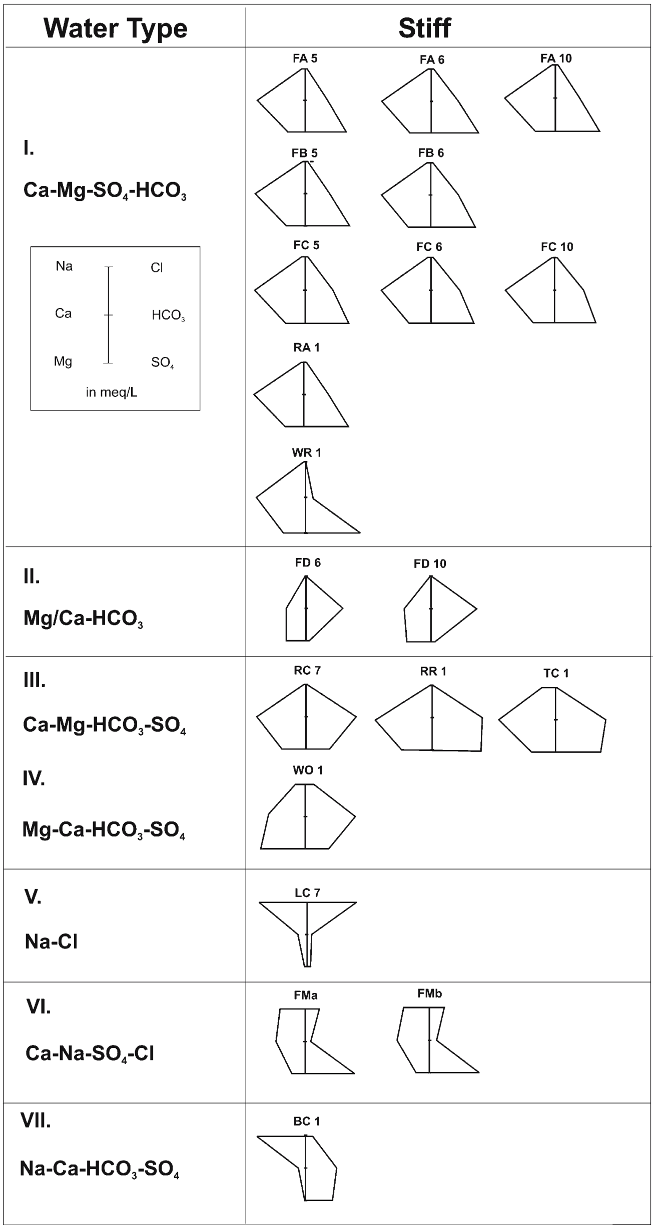

Fig. 4 Stiff diagrams and associated water types for spring waters. Ion concentrations for Stiff diagrams are plotted in milliequivalents per liter using the scale legend enclosed in the box

Types V (Na–Cl), VI (Ca–Na–SO_4–Cl) and VII (Na–Ca–HCO_3–SO_4) represented by LC, FMa and FMb, and BC, respectively, have higher Na concentrations. Anomalous high Cl levels in LC are likely related to localized evaporite deposits of the Burnais Formation which includes gypsum and anhydrites deposited in the Golden Embayment (Leech 1954). Common sinkholes in the LC area indicates active dissolution of these evaporates is occurring.

Table 3 compares the saturation index (SI) values for the various spring waters. SI values for halite (not provided) are negative as might be expected based on TDS concentrations below roughly 3,000 mg/l. However, the near-zero value for the SI of halite in LC 7 relates to the evaporite deposits encountered in this area as noted above. Calcite and dolomite are either slightly above or slightly below saturation. Without exception, gypsum is found to be under-saturated in the spring waters, and likewise, anhydrite is generally found to be under-saturated or marginally above saturation in most spring waters. In carbonate hosted springs, SO_4 may be derived from dissolution of SO_4 minerals (primarily gypsum and anhydrite) or oxidation of pyrite (secondary SO_4). As discussed below, the range of $\delta^{34}S_{(SO_4)}$ (8.9–30.4‰) (Table 2) is significantly higher than the range for sulphide minerals (Krouse 1980) indicating that SO_4 is derived from evaporate dissolution.

Table 3 Saturation indices for spring waters

Spring ID[a]	$SI_{calcite}$	$SI_{dolomite}$	SI_{gypsum}	$SI_{anhydrite}$
WO 1-2	0.0	+1.19	−1.29	−1.55
RA 1	−0.07	+0.72	−0.91	−1.04
RA 1-2	−0.16	+0.53	−0.87	−1.00
FA 5	+0.79	+2.45	−0.24	−0.37
FA 6	+0.58	+1.06	−0.29	−0.41
FA 10	+1.01	+2.97	−0.26	−0.35
FA 10-2	+0.23	+1.37	−0.29	−0.41
FB 5	+0.63	+1.98	−0.27	+0.49
FB 6	+0.08	+0.99	−0.36	−0.59
FC 5	+0.63	+2.12	−0.41	+0.56
FC 6	−0.21	+0.41	−0.50	−0.71
FC 10	+0.54	+1.98	−0.52	−0.68
FD 6	+0.13	+1.27	−2.90	−3.34
FD 10	+0.27	+1.50	−2.75	−3.21
TC 1-2	+0.07	+0.75	−0.32	−0.75
BC-2	−0.35	−0.58	−2.73	−2.96
RR 1-2	−0.39	−0.09	−0.81	−1.15
LC 7	+0.14	+1.05	−1.53	−1.67
LC 7-2	+0.01	+0.89	−1.60	−1.74
RC 7	+0.17	+1.22	−1.91	−2.11
RC 7-2	+0.24	+1.39	−2.11	−1.91
FMa	−0.07	+0.61	−0.29	−0.58
FMb	+0.25	+1.23	−0.28	−0.56
FMb-2	+0.26	+1.23	−0.27	−0.60
WR 1-2	+0.05	+0.65	−0.22	−0.51

Spring ID in Table 1

[a] Expressed as log (Ion Activity Product)/K

The degree of saturation observed in these spring waters attests to the predominance of carbonate host rocks, with water issuing from some springs possibly coming into contact with gypsum/anhydrite or halite units. As well, the SI values hint to the likelihood of forming precipitates at the spring outlets. For example, van Everdingen (1969) observed extensive spring deposits at FA and RC that, when analyzed, indicated 97 and 99%, respectively, by weight calcite. Morphological conditions (i.e., discharge into surface streams) at LC and RR springs preclude precipitation at those sites, thus SI values are not the only determining factor in forming precipitates. Changes in the concentration of dissolved CO_2 gas (resulting from off-gassing), changes in temperature that accompany discharge (usually cooling, but in the case of colder springs, a warming), and possible evaporation of spring water also play a major role in controlling precipitation conditions.

DOI 10.1007/s10040-004-0428-z

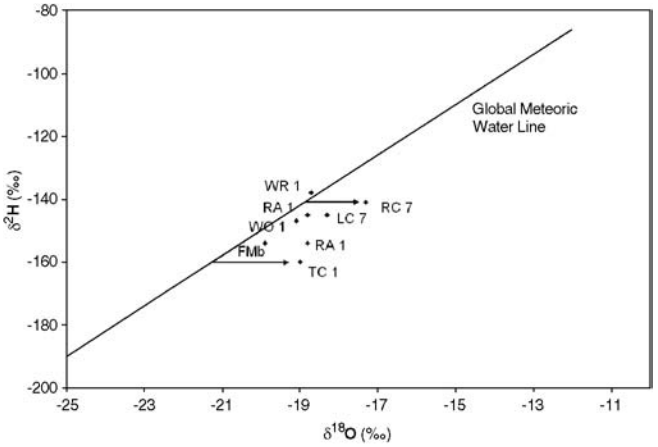

Fig. 5 δ^2H versus δ^{18}O in thermal spring waters of the Rocky Mountain Trench region. Also shown is the global meteoric water line (Craig 1961). Enrichment in δ^{18}O (*arrows*) is possibly due to thermal regime

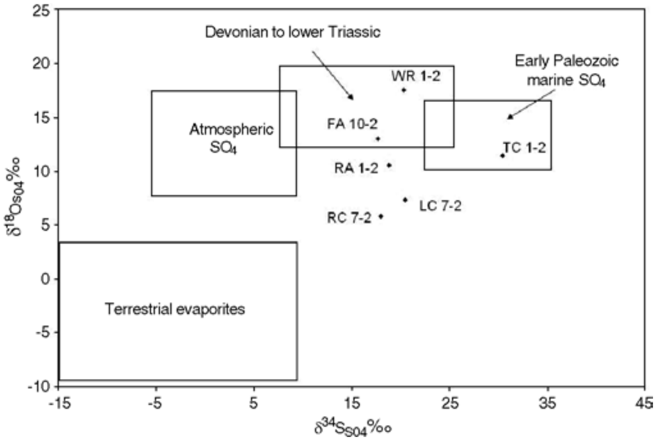

Fig. 6 δ^{34}S versus δ^{18}O in dissolved sulphate showing potential origin of sulphate in thermal spring (fields on plot modified from Clark and Fritz 1997)

Stable isotopes

Results for stable isotopes of water (δ^{18}O and δ^2H) and dissolved sulphate (δ^{34}S and δ^{18}O) are provided in Table 2. A plot of δ^{18}O versus δ^2H for thermal spring waters show they tend to fall on or to the right of the global meteoric water line (GMWL) (Craig 1961). Truesdell and Hulston (1980) showed that meteoric thermal waters are commonly altered by exchange of ^{8}O with the host rock, causing the thermal waters to shift to higher δ^{18}O values. Ghomshei and Clark (1993) demonstrated enrichment of δ^{18}O in the thermal waters of Mount Meager, British Columbia. A similar thermal enrichment is suspected to influence the isotopic composition of the Rocky Mountain Trench springs as shown in Fig. 5.

The δ^{34}S values for dissolved SO$_4$ range from 8.9 to 30.4‰ with an average of ~19‰. Springs on the east side of the RMT tend to have values close to the average. The δ^{18}O of SO$_4$ range from 5.8 to 17.5‰. The high δ^{18}O values of sulphate indicate that sulphate is derived from a primary source rather than from sulphide oxidation. This is illustrated in Fig. 6 (modified from Clark and Fritz (1997) to show spring data). No samples plot within the terrestrial evaporites field, which are derived from the oxidation of sulphides. Sample TC 1-2 plots within the Early Paleozoic marine sulphate rectangle, which encompasses marine sulphate in Ordovician and Cambrian rocks. WR 1-2 plot well within the Devonian to lower Triassic marine sulphate rectangle, which encompasses the marine sulphate in Carboniferous to Permian rocks in the region. Mixing with atmospheric sulphate originating from current day precipitation may account for the remainder of the samples. Considering that the flow systems for these springs are largely associated with Paleozoic carbonates, and that meteoric waters comprise the circulating fluid, the values are consistent with what might be expected for associated evaporite minerals. Minor alteration from the primary signature may also be the result of bacterial activity along the flow path (Grasby et al. 2000).

Table 4 Summary results of geothermometer calculations

Spring ID	Equilibration temperature (°C)
WO 1-2	28[a]
RA 1-2	59[a]
FA 10-2	52[a]
TC 1-2	90[a]
BC-2	42[a]
RR 1-2	24[b]
LC 7-2	57[a]
RC 7-2	34[a]
FMb-2	25[a]
WR 1-2	49[a]

[a] Chalcedony (Fournier 1977)
[b] Quartz (Fournier 1977)

Estimation of reservoir temperatures

All of the ion geothermometers, including Na/K (Fournier 1973), Na–K–Ca (Fournier and Truesdell 1973), Na–K–Ca with Mg correction (Fournier 1981) and Mg/Li (Kharaka and Mariner 1988) gave unrealistically high or negative equilibration temperatures; whereas the silica-based methods proved to be better suited to geological conditions. Thus, based on the temperatures calculated using each geothermometer (not provided) and the limitations of each method as discussed below, the chalcedony geothermometer was selected as the most representative. Geothermometric results are provided in Table 4. The range of equilibration temperatures for the thermal springs is between 24 and 59°C.

1. High amounts of Ca can affect the accuracy of the Na/K geothermometer at temperatures less than 180°C (Kharaka and Mariner 1988). This problem was evident by the extraordinarily high Na/K temperatures calculated for the carbonate-hosted springs in this

Table 5 Geothermal data for boreholes in the vicinity of the thermal springs in southern British Columbia

Unique hole #	Site name	Temperature log available	Thermal conductivity available	Latitude	Longitude	Total depth (m)	Gradient (°C/km)	Average thermal conductivity (W/m.K)	Heat flow (mW/m^2)
72001	Salmo	y	y	49°09	117°11	975	33.1	4.22±1.35	140
72002	Salmo	y	y	49°09	117°11	585	31.5	4.03±0.89	127
74001	Bluebell	y	y	49°45	116°51	533	55.7	2.78±0.88	155
104001	Sullivan	y	y	49°42	116°00	378	24.8	4.58±0.72	114
104002	Sullivan	y	y	49°42	116°00	320	26.7	3.38±0.64	90
104003	Sullivan	y	n	49°42	116°00	579	24.0		
104004	Sullivan	y	n	49°42	116°00	347	28.1		
104005	Sullivan	n	y	49°42	116°00	911			
104006	Sullivan	n	y	49°42	116°00	355			
104007	Sullivan	y	y	49°42	116°00	655	25.0	3.66±0.54	91
104008	Sullivan	n	y	49°42	116°00	518			
104009	Sullivan	y	y	49°42	116°00	518	27.1	3.42±0.82	93
129001	Trout Lake	y	n	50°38	117°36	523[a]	23.8		
180001	Sparwood	y	n	49°00	115°00	329[a]			
180002	Sparwood	y	n	49°00	115°00	215[a]	33.8		
180004	Sparwood	y	n	49°00	115°00	242[a]			

Location of boreholes shown in Fig. 2(*y* yes available; *n* not available)

[a] Well depths are estimated from the temperature logs

study. A possible exception of LC 7, which has an unusual Na-rich composition.

2. The Na–K–Ca (Fournier and Truesdell 1973) geothermometer, which was developed specifically to deal with Ca-rich waters that give anomalous high temperatures calculated using the Na/K method (Fournier 1981), gave unreliable results. Despite the fact that this geothermometer accounts for the effect of high Ca, the loss of Ca through calcite precipitation may have affected Na–K–Ca temperatures. Several of the sites studied had associated tufa deposits, indicating that Ca is lost from the system, and that the Na–K–Ca temperatures are unreliable.
3. The Na–K–Ca with Mg Correction (Fournier 1981) geothermometer is subject to error owing to possible continued water–rock interaction as an ascending water cools. If the Mg concentration increases as the water rises, as might occur in carbonate rocks, then application of the Mg correction will lead to anomalous low calculated reservoir temperatures.
4. For similar reasons to those above for the Na–K–Ca geothermometer, the Mg corrected Na–K–Ca geothermometer was deemed unreliable. Similarly, the Mg/Li (Kharaka and Mariner 1988) geothermometer tended to give negative values due to Mg possibly increasing during ascent.
5. The chalcedony geothermometer (Fournier 1977) is generally applicable to low-temperature thermal waters (Banks et al. 1998), although it is noted that it works best on moderate to high-temperature thermal waters (Fournier 1981). In non-quartzose rocks, the solubility of Si at temperatures below 180°C is controlled by amorphous silica and/or chalcedony (Kharaka and Mariner 1988), making the quartz geothermometer (Fournier 1977) unreliable for carbonate hosted springs. The amorphous silica geothermometer consistently gave temperatures below those measured at the surface, suggesting that the solubility of Si in carbonate hosted springs is controlled by a more stable phase like chalcedony.

Temperature gradients

Figure 7 provides examples of temperature logs at four wells (#129001, #104007, #72001 and #104003). Typically, the best estimates of the geothermal gradient are obtained from deeper wells. Many of the shallow logs (i.e., those less than 100 m) were rendered virtually useless for analysis as a result of fluid circulation in and out of the borehole due to fracturing, and near-surface thermal disturbances associated with seasonal or longer-term ground surface temperature fluctuations. As the depth of borehole increases, climate perturbations become damped and temperatures are more representative of crustal thermal conditions. Evidence of the entry and exit points for water is illustrated in the logs for hole #129001 and #104007. Water flow in nearby formations that does not enter the borehole, but influences the borehole temperature, can be only detected indirectly (Lewis et al. 1992). At Riondel (hole #74001), large amounts of hot water flowing through the underlying "Bluebell" limestone may enhance the gradient, and thus, the heat flow locally (Lewis et al. 1992). Table 5 lists a gradient value of 55.7°C/km, which is significantly higher than the gradients of the other wells. For this reason, the gradient estimate for #74001 is eliminated from the average.

The deeper sections of the temperature logs (i.e., depths greater than 200 m) were used for estimating the temperature gradients (Table 5). Gradients are relatively constant over a significant depth range, that is, gradients do not adjust according to changes in the thermal conductivity of the rocks in order to maintain a constant heat flux. This indicates a relatively uniform lithology with depth in most boreholes. The calculated gradients range

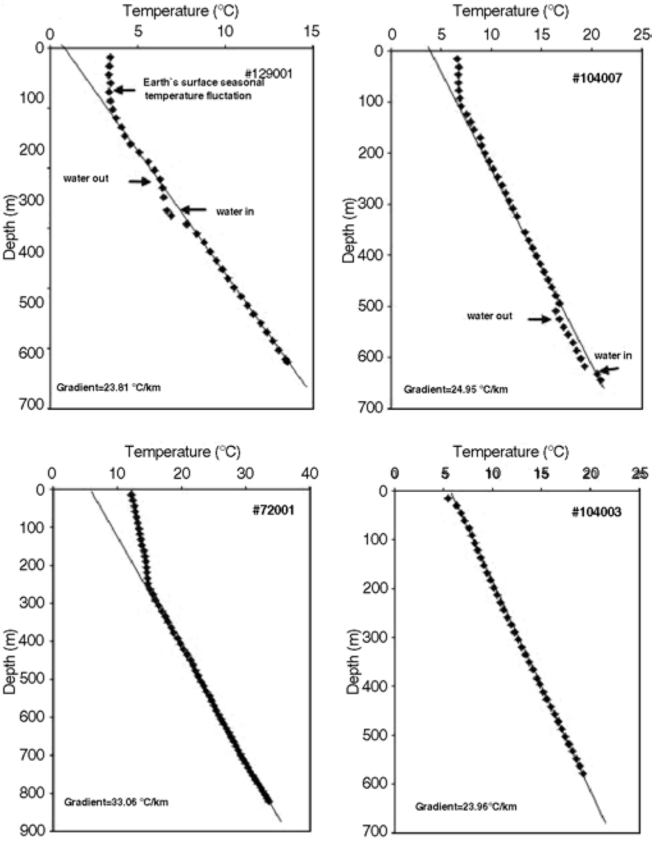

Fig. 7 Representative temperature logs obtained from boreholes of opportunity in southeastern British Columbia in the vicinity of the thermal springs investigated as part of this study. Logs demonstrate the fairly uniform geothermal gradients with depth except along sections influenced by fluid entry into and exit from the borehole. Geothermal gradients are estimated from best fit lines within suitable depth intervals. Ground surface temperatures used for calculating the depth of equilibration of spring waters are estimated by extrapolating the geothermal gradient measured at depth to ground surface. The approximate average ground surface temperature is 5°C

from 23.8 to 55.7°C/km, and excluding hole #74001 for the reasons described above, the average gradient is 24.8±8.0°C/km.

It is important to mention that extrapolation of temperature data to depths beyond those accessed by logging may introduce error in the calculated gradient. Without detailed information about the flow path of a geothermal system it would be difficult to accurately predict the true geothermal gradient, however, it will not be linear. Flow models of (Lopez and Smith 1995, 1996) indicate that complex geothermal gradients can develop locally in response to deep circulation systems. Based on their results, the depth integrated gradients vary from purely conductive heat flow by up to ~20%. If advective heat flow were significant, this would have the effect of lowering the local geothermal gradient (Forster and Smith 1988a, 1988b), making depth estimates too shallow. Thus, as with potential errors in the chalcedony geothermometers, errors in the geothermal gradient will tend to minimize depth estimates. Thus, it is presumed that the regional conductive geothermal gradient is representative within a 20% error range.

Estimation of reservoir depths

In order to estimate the depth to which the thermal spring waters circulate, two parameters need to be estimated. First is the equilibration temperature for each spring, and second is the geothermal gradient for the region. Because geothermal gradients were only available from boreholes of opportunity and these are not situated directly adjacent to the springs, the approach taken was to use the average geothermal gradient and make the assumption that it is representative of the spring region. An important limitation of applying this assumption is that most of the boreholes are located within the Omenica Tectonic Belt and not, strictly speaking, in the southern Rocky Mountains (except holes #18001–18004). However, the springs are right at the western edge of the Rocky Mountains, which coincides with the boundary of the Omenica Belt. Given the limited number of boreholes from which to estimate a gradient, it must be assumed that the average gradient for the Omenica Belt is similar to that of the southern Rocky Mountains. This assumption is at least supported by the fact that hole #18002 has a similar gradient to those measured in the other boreholes (see Table 5).

It is also important to recognize that not only might there be an error introduced by virtue of taking an average gradient, but there will likely be an error associated with the equilibration temperature. Implicit in the application of geothermometers for estimating reservoir temperatures is the fact that the waters do not come into equilibrium during their ascent from depth, and that upon ascent there is no mixing between the thermal waters and cooler shallow groundwaters with possibly a different chemical composition. Both of these factors serve to limit the strict applicability of the technique. The various geothermometers also generally result in a range of temperatures for each spring. With these limitations in mind, the approximate range of reservoir depths can be estimated.

An average ground surface temperature (approximately 5°C) was estimated by extrapolating the gradient measured at depth to ground surface for each well. Using the average geothermal gradient of 24.8°C/km and average reservoir temperatures ranging from 24 to 59°C, the reservoir depths range from 0.9 to 2.2 km. This depth range is somewhat similar to the range (0.6–1.3 km) estimated using an assumed gradient of 33°C/km with no geothermometry data to constrain the equilibration temperatures (van Everdingen 1972). Therefore, it can be concluded that the use of geothermometry, in combination with representative geothermal gradients, greatly improves the ability to estimate depths of geothermal reservoirs.

Heat flow considerations

The occurrence of thermal springs in British Columbia is generally controlled by two factors: high geothermal gradients and/or the presence of high permeability conduits (i.e., fracture zones) that extend to sufficient depths to allow for water to be heated and transported quickly to the surface. In order to speculate on the depth of origin for these thermal springs and comment on possible geologic characteristics that control their occurrence, it is important to have an understanding of the nature of the heat flow and the structural controls. However, the variety of tectonic terranes in the Canadian Cordillera that are associated with the various tectonic belts illustrated in Fig. 1 result in significant geological and structural complexity, which can lead to uncertainties in interpretation of high heat flow-related phenomena. For example, Jessop et al. (1984) stated, "The mountain zone from the Rocky Mountains to the Pacific Ocean is probably the most interesting and varied of all Canadian terrain from a geothermal point of view, and it is the most challenging in which to ensure that data truly represent the area around the site."

The thermal springs investigated in this study extend along an approximate northwest–southeast transect defined by the Rocky Mountain Trench (Fig. 1). These springs mostly issue from the sedimentary rocks forming the Foreland Fold and Thrust Belt (or the Rocky Mountain Belt). At a regional scale, the approximate linear array of the springs along the Trench edge is undoubtedly the result of northwest–southeast aligned geologic structures (Fig. 2), shown in cross section in Fig. 3. At a local scale, crustal thrust faults extending to depths of a couple of kilometers have been identified as possible conduits for flow (van Everdingen 1972).

In order to comment on the role of heat flow in the occurrence of these springs, a simplified heat flow analysis has been carried out. The geothermal database used in this study included values of thermal conductivity for several core samples that were measured using a standard divided bar apparatus (Lewis et al. 1992). Measurements on saturated core and chip samples comprise the database. In total, thermal conductivity measurements were available for 7 of the 11 boreholes (between 20 and 100 measurements per borehole). Because relatively constant geothermal gradients are measured within each borehole and a relatively low standard deviation was calculated for thermal conductivities within each borehole, an average thermal conductivity is used to estimate the heat flow for each site (Table 5).

In calculating the heat flow at each site, topographic corrections were not made; however, Lewis et al. (1992) reported using a two-dimensional finite element program to calculate the steady-state conductive topographic effects. Lewis et al. (1992) reported that the average calculated topographic correction was 33% for the entire Coast Plutonic Complex; and resulted in a lowering of the heat flow from 87.6 to 70 mW/m^2. Results from that study are compared to the current study below. Similarly, no corrections were applied for fluid flow within the boreholes because gradients were observed that are relatively uniform and undisturbed by borehole fluid circulation in the interval used to calculate the gradient.

Using the available temperature logs and measured thermal conductivity averages, heat flow values for the region range from 90 to 155 mW/m^2, with an average, based on all samples, of 116±26 mW/m^2. If borehole #74001 is eliminated from the average for the reasons discussed earlier, then the average heat flow for the region is 109±21 mW/m^2.

The average heat flow value of 109±21 mW/m^2 for this study region (based on values from six boreholes near the springs) is higher than the heat flow reported for the Omenica Belt (86±20) and for the Intermontane Belt (73±6 mW/m^2) (Lewis et al. 1992), which were based on 26 and 17 site measurements, respectively. Within the Intermontane Belt, heat flow was observed to be very uniform and moderately high, and surface heat generation is low (Lewis et al. 1992). In contrast, in the Omenica Belt, heat flow and heat generation are higher and more variable, and result in higher temperatures at shallower depths. Consequently, the Omenica Belt, and likely the areas immediately surrounding this part of the Canadian Cordillera, such as the edge of the Rocky Mountain Belt, likely experience the high temperatures to depths where faults and fracture zones remain open conduits to the surface. The high heat flow characteristics of this region in combination with well-developed geologic structure offer an explanation for the occurrence of thermal springs along the western edge of the southern Rocky Mountains.

Conclusions

The origin of thermal springs located within the southern Rocky Mountains of British Columbia was undertaken using an integrated approach involving the use of chemical geothermometers and geothermal information derived from deep boreholes. Most springs were known to have a Ca–Mg cation composition, but have variable anion composition (HCO_3-rich to SO_4-rich). Chemical geothermometers yield fairly consistent equilibration temperatures for all the springs, although only the chalcedony geothermometers provided reliable results. The equilibration temperatures for the thermal springs range from 24 to 59°C.

Geothermal gradients estimated from boreholes within the region were used in combination with the estimated reservoir temperatures to determine likely depths of circulation of the spring waters. Depths ranged from 0.9 to 2.2 km. Moderate to high heat flow and heat generation corresponding to the study region within the southern portion of the Intermontane and Omenica Belts result in generally higher temperatures at shallow depths, thus offering an explanation for the occurrence of thermal springs. The alignment of the thermal springs likely relates to the preferred northwest–southeast orientation for major thrust faults along the Rocky Mountain Trench, and source waters from depth are routed upward along deep faults.

Acknowledgements The authors would like to acknowledge the scientific contributions of Robert van Everdingen. We would also like to acknowledge the members of the Geothermal Group within the former Earth Physics Branch of Energy, Mines and Resources, Canada for their contributions to the Canadian geothermal database.

References

Armstrong RL (1988) Mesozoic and early Cenozoic magmatic evolution of the Canadian Cordillera. In: Processes in continental lithospheric deformation. Geol Soc Am Spec Pap 218:55–91

Back W (1966) Origin of hydrochemical facies in groundwater in the Atlantic Coastal Plain. In: Proceedings of International Geological Congress, Copenhagen, vol I, pp 87–95

Bally AW, Gordy PL, Stewart GA (1966) Structure, seismic data, and orogenic evolution of southern Rocky Mountains. Bull Can Petrol Geol 14:337–381

Banks D, Sletten RS, Haldorsen S, Dale B, Heim M, Swensen B (1998) The thermal springs of Bockjord, Svalbard: occurrence and major ion hydrochemistry. Geothermics 27(4):445–467

Chiba H, Sakai H (1985) Oxygen isotope exchange rate between dissolved sulphate and water at hydrothermal temperatures. Geochem Cosmochim Acta 49:993–1000

Clague JJ (1974) The St. Eugene Formation and the development of the southern Rocky Mountain Trench. Can J Earth Sci 11:916–938

Clark ID, Fritz P (1997) Environmental isotopes in hydrogeology. Lewis Publishers, New York

Coleman ML, Shepard TJ, Durham JJ, Rouse JD, Moore GR (1982) Reduction of water with zinc for hydrogen isotope analysis. Anal Chem 54:993–995

Coney PJ, Jones DL, Monger JWH (1980) Cordilleran suspect terranes. Nature 288:329–333

Craig H (1961) Isotopic variations in meteoric waters. Science 133:1702–1703

Epstein S, Mayeda TK (1953) Variation of^{18}O content of waters from natural sources. Geochim Cosmochim Acta 4:213–224

Foo WK (1979) Evolution of transverse structures linking the Purcell Anticlinorium to the western Rocky Mountains near Canal Flats, British Columbia. MSc, Queen's, Kingston, Ontario, Canada

Forster C, Smith L (1988a) Groundwater flow systems in mountainous terrain 1. Numerical modeling technique. Water Resour Res 24:999–1010

Forster C, Smith L (1988b) Groundwater flow systems in mountainous terrain 2. Controlling factors. Water Resour Res 24:1011–1023

Fournier RO (1973) Silica in thermal waters: laboratory and field investigations. In: Proceedings of International Symposium on Hydrogeochemistry and Biogeochemistry, Tokyo, pp 132–139

Fournier RO (1977) Chemical geothermometers and mixing models for geothermal systems. Geothermics 5:41–50

Fournier RO (1979) A revised equation for the Na/K geothermometer. Geotherm Resour Counc Trans 5:1–16

Fournier RO (1981) Application of water geochemistry to geothermal exploration and reservoir engineering, chap 4. In: Rybach L, Muffler LJP (eds) Geothermal systems: principles and case histories. Wiley, New York, pp 109–143

Fournier RO, Truesdell AH (1973) An empirical Na–K–Ca geothermometer for natural waters. Geochim Cosmochim Acta 37:1255–1275

Gabrielse H (1985) Major dextral transcurrent displacements along the northern Rocky Mountain trench and related lineaments in north-central British Columbia. Geol Soc Am Bull 96:1–14

Gabrielse H, Yorath CJ (1989) DNAG No. 4. The Cordilleran Orogen in Canada. Geosci Can 16:67–83

Ghomshei MM, Clark ID (1993) Oxygen and hydrogen isotopes in deep thermal waters from the South Meager Creek geothermal area, British Columbia, Canada. Geothermics 22(2):79–89

Grasby SE, Hutcheon I (2001) Controls on the distribution of thermal springs in the southern Canadian Cordillera. Can J Earth Sci 38(3):427–440

Grasby SE, Hutcheon I, Krouse HR (2000) The influence of water–rock interaction on the chemistry of thermal springs in western Canada. Appl Geochem 15:439–454

Hitchon B (1984) Geothermal gradients, hydrodynamics, and hydrocarbon resources, Alberta, Canada. Am Assoc Petrol Geol J 68:713–743

Hyndman RD, Yorath CJ, Clowes RM, Davis EE (1990) The northern Cascadia subduction zone at Vancouver Island: seismic structure and tectonic history. Can J Earth Sci 27:313–329

Jessop AM, Lewis TJ, Judge AS, Taylor AE, Drury MJ (1984) Terrestrial heat flow in Canada. Tectonophysics 103:239–261

Kharaka YK, Mariner RH (1988) Chemical Geothermometers and their application to formation waters from sedimentary basins. In: Thermal history of sedimentary basins; methods and case histories. Springer, Berlin Heidelberg New York, pp 99–8117

Krouse HR (1980) Sulphur isotopes in our environment. In: Fritz P, Fontes JC (eds.), Handbook of Environmental Isotope Geochemistry, Vol. 1., The Terrestrial Environment. Elsevier, Amsterdam, pp. 435–471

Leech GB (1954) Canal Flats, British Columbia. Geological Survey of Canada, Canada

Lewis TJ, Souther JG (1978) Meager Mountain, B.C.—a possible geothermal energy resource. Earth Physics Branch, Energy Mines and Resources Canada

Lewis TJ (1991) Heat flux in the Canadian Cordillera. In: The Neotectonics of North America. Decade of North American Geology. Geol Soc Am, pp 445–456

Lewis TJ, Benthowski WH, Hyndman RD (1992) Crustal temperatures near the Lithoprobe Southern Canadian Transect. Can J Earth Sci 29:1197–1214

Lopez DL, Smith L (1995) Fluid flow in fault zones; analysis of the interplay of convective circulation and topographically driven groundwater flow. Water Resour J 187:71–87

Lopez DL, Smith L (1996) Fluid flow in fault zones; influence of hydraulic anisotropy and heterogeneity on the fluid flow and heat transfer regime. Water Resour Res 32(10):3227–3235

Mizutani Y, Rafter TA (1969) Oxygen isotopic composition of sulphates, 3. Oxygen isotopic fractionation in the bisulfate ion-water system. New Zealand J Sci 12:54–59

Monger JWH, Price RA, Templeman-Kluit DJ (1982) Tectonic accretion and the origin of the two major metamorphic and plutonic belts in the Canadian Cordillera. Geology 10:70–75

Parrish RR, Carr SD, Parkinson DL (1988) Eocene extensional tectonics and geochronology of the southern Omenica Belt, British Columbia and Washington. Tectonics 7:181–212

Price RA (1962) Fernie map-area, east half, Alberta and British Columbia. Geological Survey of Canada, Canada

Price RA, Carmichael DM (1986) Geometric test for Late Cretaceous-Paleogene intracontinental transform faulting in the Canadian Cordillera. Geology 14(6):468–471

Satterley J, Elworthy RT (1917) Mineral springs of Canada, Part I—The radioactivity of some Canadian mineral springs. Can Mines Branch Bull 16:60

Shakur A (1982) ^{34}S and^{18}O variations in terrestrial sulphates. PhD thesis, University of Calgary, Alberta, Canada

Souther JG (1976) Geothermal potential of western Canada. In: Proceedings of 2nd United Nations Symposium on the Development and Use of Geothermal Resources, San Francisco, CA, vol 1, pp 259–267

Souther JG, Halstead EC (1973) Mineral and thermal waters of Canada. Department of Energy, Mines and Resources Canada

Souther JG, Dellechaie F (1984) Geothermal exploration at Mt. Cayley—a quaternary volcano in southwestern British Columbia. Geotherm Resour Counc Trans 6:463–468

Stiff HJ Jr (1951) The interpretation of chemical water analysis by means of patterns. J Petrol Technol 3:15–17

Truesdell AH, Hulston JR (1980) Isotopic evidence of environments of geothermal systems. In: Fritz P, Fontes JC (eds) Handbook of environmental isotope chemistry, vol. 1. Elsevier, New York, pp 179–226

van der Velden AJ (1995) Subsurface geometry and tectonic controls on the development of the Rocky Mountain trench in southeastern British Columbia, Canada. Unpublished MSc, University of Calgary, Calgary Alberta, 91 pp van der Velden AJ, Cook FA (1994) Displacement of the Lewis thrust sheet in the southwestern Cordillera: new evidence from seismic reflection data. Geology 22:819–822

van Everdingen RO (1969) Degree of saturation with respect to $CaCO_3$, $CaMg(CO_3)_2$, and $CaSO_4$ for some thermal and mineral springs in the Southern Rocky Mountains, Alberta and British Columbia. Can J Earth Sci 6:1421–1430

van Everdingen RO (1972) Thermal and mineral springs in the southern Rocky Mountains of Canada. Water Management Service Department of the Environment, Ottawa, Ontario, Canada

Wiwchar B, Perkins EH, Gunter WD (1988) SOLMINEQ.88 PC/SHELL manual. Alberta Research Council, Oil Sands and Hydrocarbon Recovery Department

Woodsworth G (1999) Hot springs of western Canada: a complete guide. 2nd edn. Gordon Soules Publishers, West Vancouver, 288 pp

Yanagisawa F, Sakei H (1983) Precipitation of SO_2 for sulphur isotopic ratio measurements by thermal decomposition of $BaSO_4$–V_2O_5–SiO_2 mixtures. Anal Chem 55:985–987

Yorath CJ, Gordy PL, Williams GK, Bustin RM, Bell RT, Souther JG, Halstead EC (1991) Energy and ground water resources of the Canadian Cordillera, chap 20. In: Gabrielse H, Yorath CJ (eds) Geology of the Cordilleran Orogeny in Canada, vol 4. Geol Surv Can, Geology of Canada, pp 769–801

DOI 10.1007/s10040-004-0428-z